What is LiFi?

Harald Haas, *Member, IEEE*, Liang Yin, *Student Member, IEEE*, Yunlu Wang, *Student Member, IEEE*, and Cheng Chen, *Student Member, IEEE*

***Abstract*—This paper attempts to clarify the difference between visible light communication (VLC) and light-fidelity (LiFi). In particular, it will show how LiFi takes VLC further by using light emitting diodes (LEDs) to realise fully networked wireless systems. Synergies are harnessed as luminaries become LiFi attocells resulting in enhanced wireless capacity providing the necessary connectivity to realise the Internet-of-Things, and contributing to the key performance indicators for the fifth generation of cellular systems (5G) and beyond. It covers all of the key research areas from LiFi components to hybrid LiFi/wireless fidelity (WiFi) networks to illustrate that LiFi attocells are not a theoretical concept any more, but at the point of real-world deployment.**

***Index Terms*—Base stations, communication networks, communication systems, handover, millimeter wave communication, mobile communication, modulation, multiaccess communication, wireless communication.**

I. Introduction

DUE to the increasing demand for wireless data communication, the available radio spectrum below 10 GHz (cm-wave communication) has become insufficient. The wireless communication industry has responded to this challenge by considering the radio spectrum above 10 GHz (mm-wave communication). However, the higher frequencies, f, mean that the path loss, L, increases according to the Friis free space equation ($L \propto f^2$). In addition, blockages and shadowing in terrestrial communication are more difficult to overcome at higher frequencies. As a consequence, systems must be designed to enhance the probability of line-of-sight (LoS), typically by using beamforming techniques and by using very small cells (about 50 m in radius). The need for small cells is not an issue from a system capacity perspective. This is because reducing cell sizes has without doubt been the major contributor for enhanced system performance in current cellular communications. This means, contrary to the general understanding, using higher frequencies for terrestrial communication has become a practical option. However, one disadvantage is that the challenge for providing a supporting infrastructure for ever smaller cells becomes significant. One such example is the provision of a sophisticated backhaul infrastructure. Light-fidelity (LiFi) [1], [2] is a continuation of the trend to move to higher frequencies in the electromagnetic spectrum. Specifically, LiFi could be classified as nm-wave communication. LiFi uses light emitting diodes (LEDs) for high speed wireless communication, and speeds of over 3 Gb/s from a single micro-light emitting diode (LED) [3] have been demonstrated using optimised direct current optical orthogonal frequency division multiplexing (DCO-OFDM) modulation [4]. Given that there is a widespread deployment of LED lighting in homes, offices and streetlights because of the energy-efficiency of LEDs, there is an added benefit for LiFi cellular deployment in that it can build on existing lighting infrastructures. Moreover, the cell sizes can be reduced further compared with mm-wave communication leading to the concept of LiFi attocells [5]. LiFi attocells are an additional network layer within the existing heterogeneous wireless networks, and they have zero interference from, and add zero interference to, the radio frequency (RF) counterparts such as femtocell networks. A LiFi attocell network uses the lighting system to provide fully networked (multiuser access and handover) wireless connectivity.

This paper is an extension of an invited paper [6] at European Conference on Optical Communication 2015. It takes a broader view in order to appropriately define LiFi, and to contrast it to well-established related concepts such as visible light communication (VLC). To the authors' best knowledge, along with [6] this is the first time that such clarification is provided. Therefore, the papers starts by discussing key research areas that are relevant to LiFi. The areas that VLC and LiFi have in common such as digital modulation techniques are addressed in a tutorial manner, while the areas that are unique to LiFi are discussed in more detail and technical solutions are provided and discussed in sufficient depth in order to support the results provided therein. Because of the deliberate breadth of this paper and the limited space, the interested reader will also be provided with references for a more in-depth study of the techniques discussed in this paper. The rest of the paper is structured as follows: In Section II, the key differences between VLC and LiFi are discussed. A summary of state-of-the-art modulation techniques used in LiFi systems is provided in Section III. In Section IV, the first LiFi transmitter and receiver application-specific integrated circuits (ASICs) components are introduced. In Section V, an important element of a full LiFi network, namely multiuser access techniques are discussed. In Section VI, LiFi attocell networks are modelled, including the consideration of co-channel interference (CCI). In Section VII, hybrid LiFi and Wireless-Fidelity (WiFi) networks are analysed and it is shown that both systems can gain from each other. Finally, conclusions are given in Section VIII.

II. LiFi Versus VLC

VLC uses LEDs to transmit data wirelessly by using intensity modulation (IM). At the receiver the signal is detected by a

Manuscript received October 25, 2015; revised December 3, 2015; accepted December 7, 2015. The work of Prof. H. Haas was supported by the EPSRC under Established Career Fellowship Grant EP/K008757/1.

The authors are with the Li-Fi Research and Development Centre, Institute for Digital Communications, The University of Edinburgh, Edinburgh EH9 3JL, U.K. (e-mail: h.haas@ed.ac.uk; l.yin@ed.ac.uk; yunlu.wang@ed.ac.uk; cheng.chen@ed.ac.uk).

Color versions of one or more of the figures in this paper are available online at http://ieeexplore.ieee.org.

Digital Object Identifier 10.1109/JLT.2015.2510021

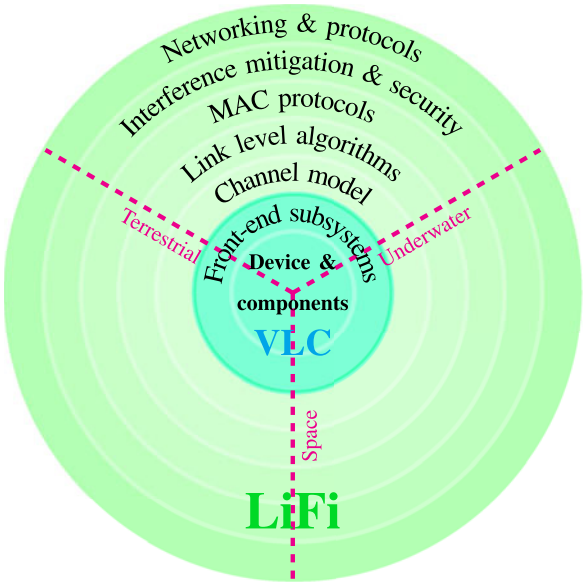

Fig. 1. The principal building blocks of LiFi and its application areas.

photodiode (PD) and by using the principle of direct detection (DD). VLC has been conceived as a point-to-point data communication technique – essentially as a cable replacement. This has led to early VLC standardisation activities as part of IEEE 802.15.7 [7]. This standard, however, is currently being revised to include LiFi. LiFi in contrast describes a complete wireless networking system. This includes bi-directional multiuser communication, i.e. point-to-multipoint and multipoint-to-point communication. LiFi also involves multiple access points forming a wireless network of very small optical attocells with seamless handover. This means that LiFi enables full user mobility, and therefore forms a new layer within the existing heterogeneous wireless networks. The fact that LEDs are natural beamformers enables local containment of LiFi signals, and because of the blockage of the signals by opaque walls, CCI can effectively be managed and physical layer security can be enhanced. Fig. 1 illustrates the principal techniques that are needed to create optical attocell LiFi networks. At the core are novel devices such as gallium nitride (GaN) micro-LEDs and single photon avalanche diodes. These are embedded in optical front-ends and subsystems which include adaptive optics and also the analogue circuitry to drive the LEDs and shape the signals obtained from the PDs at the receivers. In order to correctly model link margins, establish the coherence bandwidth of the channel and correctly model CCI, precise channel models are required which take the spectral composition of the signal into account [8]. Link level algorithms are required to optimally shape the signals to maximise the data throughput. In this context, due to the positivity of the power signals in IM, a new theoretical framework is needed to establish the channel capacity since the traditional Shannon framework is not strictly applicable [9]. In order to enable multiuser access, new medium access control (MAC) protocols are required that take the specific features of the LiFi physical layer into account. Similarly, interference mitigation techniques are needed to ensure fairness and high overall system throughput. Lastly, the optical attocell network should be integrated into software defined networks governed by the separation of the control and data planes as well as network virtualization [10]. This requires the development of novel LiFi agents. There has been significant research activity around the inner two layers which form VLC, but little research in remaining areas including channel modelling where recently, however, significant activity has been seen.

III. Modulation Techniques for LiFi

In this section, digital modulation techniques generally used for LiFi are summarised, and some special issues and requirements are discussed. In principle, LiFi also relies on electromagnetic radiation for information transmission. Therefore, typically used modulation techniques in RF communication can also be applied to LiFi with necessary modifications. Moreover, due to the use of visible light for wireless communication, LiFi also provides a number of unique and specific modulation formats.

A. Single-Carrier Modulation (SCM)

Widely used SCM schemes for LiFi include on-off keying (OOK), pulse position modulation (PPM) and pulse amplitude modulation (PAM), which have been studied in wireless infrared communication systems [11]. OOK is one of the well known and simple modulation schemes, and it provides a good trade-off between system performance and implementation complexity. By its very nature that OOK transmits data by sequentially turning on and off the LED, it can inherently provide dimming support.[1] As specified in IEEE 802.15.7 [12], OOK dimming can be achieved by: i) refining the ON/OFF levels; and ii) applying symbol compensation. Dimming through refining the ON/OFF levels of the LED can maintain the same data rate, however, the reliable communication range would decrease at low dimming levels. On the other hand, dimming by symbol compensation can be achieved by inserting additional ON/OFF pulses, whose duration is determined by the desired dimming level. As the maximum data rate is achieved with a 50% dimming level assuming equal number of 1 and 0 s on average, increasing or decreasing the brightness of the LED would cause the data rate to decrease.

Compared with OOK, PPM is more power-efficient but has a lower spectral efficiency. A variant of PPM, termed variable pulse position modulation (VPPM) [12], can provide dimming support by changing the width of signal pulses, according to a specified brightness level. Therefore, VPPM can be viewed as a combination of PPM and pulse width modulation (PWM). A novel SCM scheme, termed optical spatial modulation [13], which relies on the principle of spatial modulation, proves to be both power- and bandwidth-efficient for indoor optical wireless

[1] In general, there are two main approaches to dim LEDs: analogue dimming and digital dimming. Since this section is focused on modulation schemes in LiFi, only modulation-based digital dimming schemes are discussed.

communication. As a variant of quadrature amplitude modulation (QAM) for single carrier systems, carrier-less amplitude and phase modulation [14] uses two orthogonal signals, in place of the real and imaginary parts of the QAM signaling format, for spectrum-efficient signal transmission in LiFi networks.

B. Multi-Carrier Modulation

As the required data rate increases in LiFi networks, SCM schemes such as OOK, PPM and PAM start to suffer from unwanted effects, such as non-linear signal distortion at the LED front-end and inter-symbol interference caused by the frequency selectivity in dispersive optical wireless channels. Therefore, for high-speed optical wireless communication, efforts are drawn to multi-carrier modulation (MCM). Compared with SCM, MCM is more bandwidth-efficient but less energy-efficient. One and perhaps the most common realisation of MCM in LiFi networks is OFDM [15], [16], where parallel data streams are transmitted simultaneously through a collection of orthogonal subcarriers and complex equalization can be omitted. If the number of orthogonal subcarriers is chosen so that the bandwidth of the modulated signal is smaller than the coherence bandwidth of the optical channel, each sub-channel can be considered as a flat fading channel. Techniques already developed for flat fading channels can therefore be applied. The use of OFDM allows for further adaptive bit and power loading techniques on each subcarrier so that enhanced system performance can be achieved. An OFDM modulator can be implemented by an inverse discrete Fourier transform block, which can be efficiently realised using the inverse fast Fourier transform (IFFT), followed by a digital-to-analogue converter (DAC). As a result, the OFDM-generated signal is complex and bipolar by nature. In order to fit the IM/DD requirement imposed by commercially available LEDs, necessary modifications to the conventional OFDM techniques are required for LiFi.

The commonly used method for ensuring a real-valued signal output after IFFT is by enforcing Hermitian symmetry on the subcarriers. Moreover, as the light intensity cannot be negative, the LiFi signal needs to be unipolar. There are many methods to obtain a unipolar time-domain signal. DCO-OFDM [11] uses a positive direct current (DC) bias for unipolar signal generation. This method brings an increase in the total electrical power consumption, but without further loss in spectral efficiency. Asymmetrically clipped optical OFDM (ACO-OFDM) [17] is another type of optical OFDM scheme where, as well as imposing Hermitian symmetry, only the odd subcarriers are used for data transmission and the even subcarriers are set to zero. Therefore, the spectral efficiency of ACO-OFDM is further halved. Since only a small DC bias is required in ACO-OFDM, it is more energy-efficient than DCO-OFDM. Asymmetrically clipped direct current biased OFDM (ADO-OFDM) [18] is a combination of DCO-OFDM and ACO-OFDM, where the DCO-OFDM scheme is used on the even subcarriers and the ACO-OFDM scheme is used on the odd subcarriers. In certain scenarios, it is shown that ADO-OFDM outperforms both DCO-OFDM and ACO-OFDM in terms of power-efficiency. To incorporate dimming support into optical OFDM, reverse polarity optical OFDM (RPO-OFDM) [19] was proposed to combine the high rate OFDM signal with the slow rate PWM signal, both of which contribute to the overall illumination of the LED. Since RPO-OFDM fully utilizes the linear dynamic range of the LED, non-linear signal distortion is minimised. Another modulation scheme, termed PAM discrete multitone modulation [20], also clips the entire negative signal as in ACO-OFDM. The difference is that pulse-amplitude-modulated discrete multitone modulation (PAM-DMT) uses all of the available subcarriers for information transmission, however, only the imaginary parts of the signal are modulated on each subcarrier. In this way, signal distortion caused by asymmetric clipping falls on the real component, and is orthogonal to the information-carrying signal. A hybrid optical OFDM scheme combining ACO-OFDM and PAM-DMT, termed asymmetrically hybrid optical OFDM (AHO-OFDM) [21], uses both odd and even subcarriers for information transmission. In AHO-OFDM, dimming capability is supported by a DC bias without a further requirement of the commonly used PWM technique. The fact that compact multi-LED arrays can be realised straightforwardly has led to a new OFDM technique that assigns subcarriers to physically separated LEDs in an array [22]. This helps mitigate non-linear distortions due to high peak-to-average power ratio in OFDM.

As an alternative to ACO-OFDM, flip-OFDM [23] and unipolar OFDM (U-OFDM) [24] can achieve comparable bit error ratio (BER) performance and spectral efficiency. A novel modulation scheme, named enhanced unipolar OFDM (eU-OFDM) [25], allows a unipolar signal generation without additional spectral efficiency loss as in ACO-OFDM, PAM-DMT, flip-OFDM and U-OFDM. Recently, an alternative to OFDM has been proposed [26], which uses the Hadamard matrix instead of the Fourier matrix as an orthogonal matrix to multiplex multiple data streams.

C. LiFi Specific Modulation

LiFi transmitters are generally designed not only for wireless communication but also for illumination, which can be realised either by using blue LEDs with yellow phosphorus coating or by colour mixing through coloured LEDs. Luminaires equipped with multicoloured LEDs can provide further possibilities for signal modulation and detection in LiFi systems [27].

Color shift keying (CSK) is an IM scheme outlined in IEEE 802.15.7 [12], where signals are encoded into colour intensities emitted by red, green and blue (RGB) LEDs. In CSK, incoming bits are mapped on to the instantaneous chromaticities of the coloured LEDs while maintaining a constant average perceived colour. The advantages of CSK over conventional IM schemes are twofold. Firstly, since a constant luminous flux is guaranteed, there would be no flicker effect over all frequencies. Secondly, the constant luminous flux implies a nearly constant LED driving current, which reduces the possible inrush current at signal modulation, and thus improves LED reliability. Based on CSK, metameric modulation (MM) [28] was developed and it can achieve higher energy efficiency and provide further control of the colour quality, however, with the disadvantage of requiring an additional and independently controlled green LED.

From the perspective of maximising the communication capacity, colour intensity modulation (CIM) is proposed in [29]. For both orthogonal and non-orthogonal optical channels.

IV. LiFi Components

A key to the commercial adoption of LiFi in applications such as the Internet-of-Things (IoT), 5th generation of cellular systems (5G) and beyond, light as a service in lighting, car-to-car communication, security and defence, underwater communication and wireless interconnects in data centres, is the availability of low cost and low power miniaturised transceiver technology. It is therefore essential to develop LiFi ASICs. In this section, to the authors' best knowledge, a first transmitter ASIC and receiver ASIC based on complementary metal oxide semiconductor (CMOS) technology are presented. Both chips have recently been developed as part of the UK Engineering and Physical Sciences Research Council (EPSRC) ultra-parallel visible light communication (UPVLC) project.

A. Transmitter Chip

Conventional circuits that support OFDM or PAM involve a DAC to generate high-speed signals. Typical DAC structures can only deliver up to $30\ \mathrm{mA}$ current [30], and they require an additional stage of current amplifier in order to drive a typical LED. An open-drain 8-bit current steering DAC-based LED driver using CMOS technology has been developed in [31], and it omits the additional current amplifier. The layout and package of the chip are shown in Fig. 2(a) and (b), respectively. The ASIC is capable of achieving $250\ \mathrm{MS/s}$ at a maximum full-scale current of $255\ \mathrm{mA}$ and exhibits a power efficiency of 72%. A differential optical drive is implemented by employing both current steering branches of the DAC to drive two different colour LEDs. This doubles the signal level and efficiency over a single ended approach, and enables the transmitter configuration described in [32]. The chip has four separate driver channels. Each channel is capable of driving up to two LEDs allowing for CSK, lighting colour-temperature adjustment and a multiple input multiple output (MIMO) system.

An analysis of the BER as a function of measured signal-to-noise ratio (SNR) at different full-scale currents is shown in Fig. 3. An uncoded OFDM signal is used in the experiment. The distance between the LED and the receiver is $1\ \mathrm{m}$. As expected, an increase in the full-scale current results in a higher optical output power and, hence, higher SNR at the receiver. The system is subject to non-linear distortions at the transmitter and the receiver. Therefore, an SNR of about $25\ \mathrm{dB}$ is required to achieve an uncoded BER of 10^{-3}. As shown in Fig. 3, the BER does not improve when the current reaches about $250\ \mathrm{mA}$ due to saturation effects. It has been shown that it is possible to transmit $1\ \mathrm{Gb/s}$ when using all four drivers in parallel in a MIMO configuration [33].

B. Receiver Chip

LiFi systems are based on IM/DD. As a consequence, the average transmit power is proportional to the transmit signal amplitude, and not the square of the signal amplitude. The electrical path loss is hence twice the optical path loss. Therefore, in order to achieve reasonable distances in an attocell network, receiver devices with sufficiently high sensitivity are required. Based on computer modelling, it is indicated in [33] that an avalanche photodetector (APD)-based receiver with a typical input referred noise density of $10\ \mathrm{pA}/\sqrt{\mathrm{Hz}}$ is necessary for reliable communication. A LiFi receiver chip composed of 49 APD

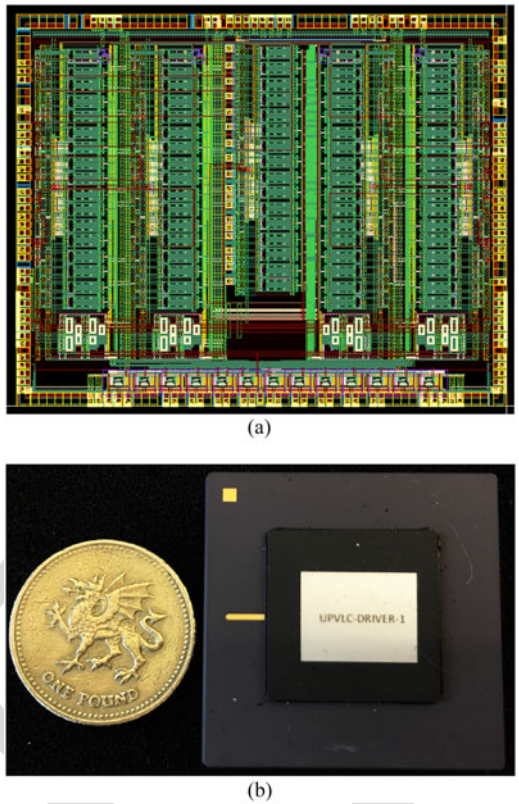

Fig. 2. LiFi transmitter chip – developed within UPVLC project. (a) Layout of LiFi driver chip in CMOS. (b) Packaged LiFi driver chip (size: $3.3 \times 3.3\ \mathrm{cm}^2$ — the actual silicon die is $5\ \mathrm{mm} \times 6\ \mathrm{mm}$), with a coin alongside to give the scale.

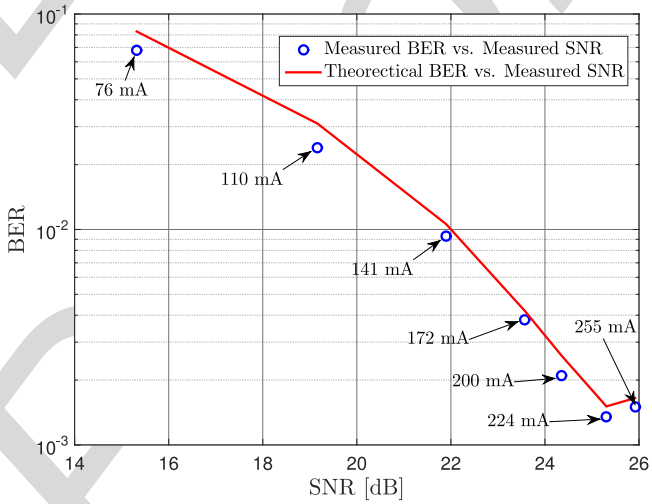

Fig. 3. BER of the DAC in the CMOS transmitter chip.

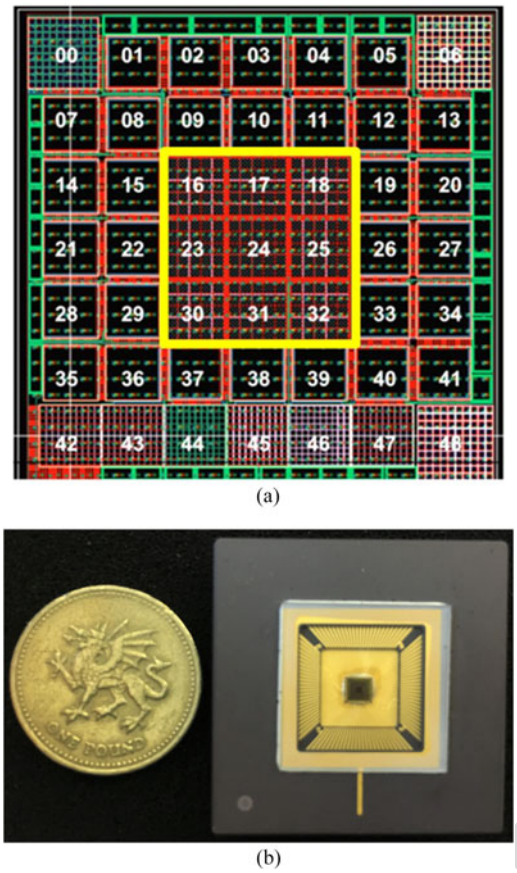

Fig. 4. LiFi receiver chip – developed within UPVLC project. (a) Layout of LiFi receiver chip with 49 APD detectors on CMOS. (b) Packaged LiFi receiver chip (size: 3.3×3.3 cm^2— the actual silicon die is 3 mm $\times$ 3 mm), with a coin alongside to give the scale.

detectors (a 7×7 detector array) based on 180 μm CMOS technology has been developed (see Fig. 4). The size of each APD element is 200 μm $\times$ 200 μm placed on a 240 μm grid. The responsivity of the nine APDs at the central core is 2.61 A/W at 450 nm. An APD gain of 10 dB is achieved at a reverse bias voltage of only 10 V. Each APD is connected to an integrated transimpedance amplifier based on a shunt-shunt feedback topology with fixed gain in order to obtain good performance. The APDs achieve a bandwidth of 90 MHz. The APDs outside the central core exhibit different colour sensitivities. Also, there are several APDs at the fringe (numbers 6, 8 and 42–48) that are exposed to a specially designed metal grading structure to achieve enhanced directionality for angular diversity receiver algorithms [34].

V. Multiuser Access in LiFi

As a wireless broadband technology, LiFi can provide multiple users with simultaneous network access. In previous research [35], optical space division multiple access (SDMA) has been studied by using an angle diversity transmitter. When compared with the optical time division multiple access (TDMA) technique, it has been shown that optical SDMA can achieve more than tenfold increase in the system throughput within a LiFi network. However, such performance enhancement requires careful design of the angle diversity transmitter and time-consuming user-grouping algorithms based on exhaustive search. OFDM provides a straightforward method for multiuser access, i.e., orthogonal frequency division multiple access (OFDMA), where users are served and separated by a number of orthogonal subcarriers. However, unlike RF systems, no fast fading exists in LiFi systems and the indoor optical wireless channel shows the characteristic similar to the frequency response of a low-pass filter. Hence, subcarriers with lower frequencies generally provide users with high SNR statistics. Therefore, it is important in OFDMA to use appropriate user-scheduling techniques to ensure that fairness in the allocation of resources (subcarriers) is maintained.

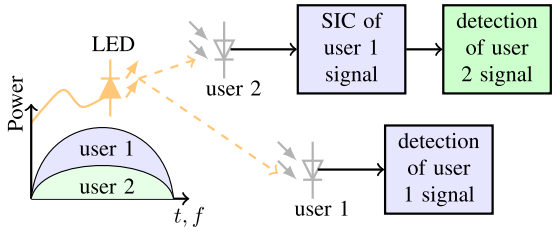

Fig. 5. Illustration of NOMA principle (two-user example).

In order to enhance the throughput of cell edge users, non-orthogonal multiple access (NOMA) was proposed in [36] for RF communication systems. By utilizing the broadcasting nature of LEDs, it was shown in [37] that the performance of a LiFi network can be efficiently enhanced with the application of NOMA. Different from conventional orthogonal multiple access technologies, NOMA can serve an increased number of users via non-orthogonal resource allocation (RA), and it is considered as a promising technology for 5G wireless communication [38]. There are various multiplexing schemes for NOMA, however, in this paper the focus is on a single variant, namely power-domain multiplexing. In this scheme, successive interference cancellation (SIC) is used at the receiver side to cancel the inter-user interference.

A. Multiuser Access in Single LiFi attocell

The basic principle of downlink NOMA is shown in Fig. 5, where the LED broadcasts a superpositioned version of the messages intended for a group of users of interest. Based on power-domain multiplexing, the superpositioned signal is given as a summation of signals, with each multiplied by a weighing factor. Due the fact that the indoor LoS channel is largely deterministic and strongly related to the Euclidean distance of the transmission link, the channel qualities or the signal-to-interference-plus-noise ratios (SINRs) may fluctuate significantly among users. For this reason, the interfering signal is detected and canceled in a descending order of the SINR at each receiver (excluding the user with the worst channel quality). Furthermore, in the process of signal detection, the interfering signals whose power are smaller than the useful signal power are treated as noise.

Consider the downlink LiFi transmission in a single attocell, in which the optical access point (AP) is located in the ceiling and K mobile users are uniformly scattered within a disc underneath. Without loss of generality, all of the users are first indexed based on their channel conditions, so that $h_1 \leq \cdots \leq h_k \leq \cdots \leq h_K$, where h_k represents the optical

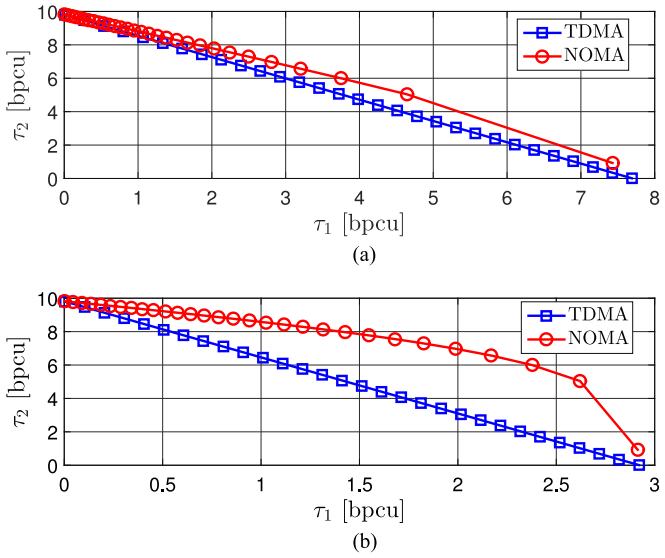

Fig. 6. Shannon spectral efficiency comparison between NOMA and TDMA in a LiFi attocell setup (two-user example): (a) two users with similar channel conditions; (b) two users with distinctive channel conditions.

TABLE I

Parameters	Values
Vertical separation	2.25 [m]
PD responsivity	0.6 [A/W]
PD physical area	1 [cm^2]
Receiver FoV	90°
Receiver noise PSD	10^{-19} [A^2/Hz]

channel gain between the k-th user and the LiFi AP. In order to balance user data rate regardless of their geographical locations, the power partition parameters, denoted by a_k, are set so that users with poorer channel equalities are allocated more signal power ($a_1 \geq \cdots \geq a_k \geq \cdots \geq a_K$), at the same time satisfying the total power constraint. Assuming perfect knowledge of the channel state information (CSI) and SIC signal processing at the receiver side, the Shannon limit on spectral efficiency for each user, denoted by τ_k, can be found as:

$$\tau_k = \begin{cases} \log_2\left(1 + \dfrac{(h_k a_k)^2}{\sum_{i=k+1}^{K}(h_k a_i)^2 + \frac{1}{\rho}}\right), & k \neq K \\ \log_2\left(1 + \rho(h_k a_k)^2\right), & k = K \end{cases} \quad (1)$$

where ρ represents the transmit SNR at the LiFi AP.

As shown in Fig. 6, the performance of NOMA is simulated in a LiFi attocell setup with two users. The parameters listed in Table I are used. It can be seen from Fig. 6 that, when compared with the conventional TDMA technique, NOMA can always increase the sum throughput of LiFi networks. Also, from the slope of the curves, it can be found that NOMA can further enhance the performance of users at the cell edge, without significantly deteriorating the performance of other users with better channel qualities.

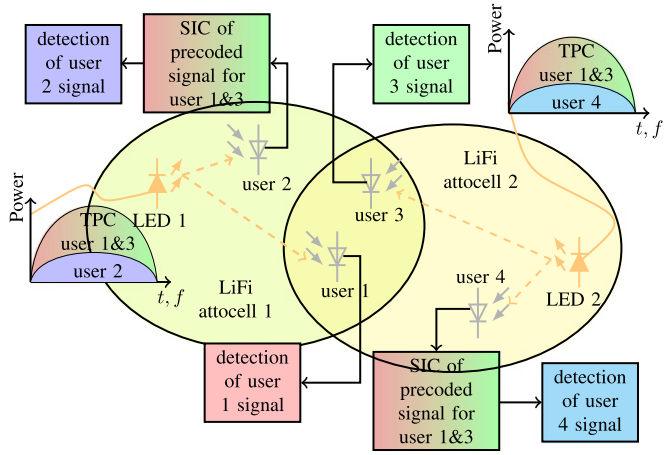

Fig. 7. Illustration of combined use of NOMA and SDMA in a two-cell LiFi network. SIC is used to eliminate interference.

B. Multiuser Access in LiFi Attocell Networks

In the first part of this section, the application of NOMA in a single LiFi attocell configuration is discussed. In the second part, the application of NOMA in a LiFi network is discussed. Due to the overlapping coverage area of adjacent LiFi APs, the cell edge users will experience increased interference from neighbouring attocells. As shown in Fig. 7, cell edge user 1 in LiFi attocell 1 also receives the unwanted signal transmitted from the AP in LiFi attocell 2. Therefore, directly using NOMA in a LiFi network cannot efficiently mitigate interference transmitted from adjacent attocells. This inter-cell interference can be efficiently reduced or mitigated through intelligent frequency planning techniques, however, with the disadvantage of reducing the frequency utilisation efficiency. One promising and effective solution to enhance the performance of cell edge users in a LiFi network is the combination of NOMA and SDMA. Unlike [35], where SDMA is realised with the use of an angle diversity transmitter, in this paper SDMA is based on a coordinated multi-point (CoMP)-aided joint transmission technique. Specifically, users at different locations are served simultaneously with the use of transmit pre-coding (TPC). After the signal propagating through the optical channel to the receiver side, inter-user interference is mitigated aided by TPC and SDMA. Take Fig. 7 as an example, since user 1 and user 3 can receive signals from both LED 1 and LED 2, their "spatial signatures," i.e., optical channel gains, are exploited for designing the TPC vector. As a result, transmission links from both LEDs are added constructively to help enhance the performance of user 1 and user 3 at the cell edge. CoMP-aided SDMA requires the LiFi APs to have knowledge of both the message data and CSI of user 1 and user 3. Note that in such a LiFi network, only the cell edge users are coordinated for joint transmission. Therefore, the added signaling overhead and complexity in exchange for enhanced system performance are not significant. Different from Fig. 5, where only user 2 needs to cancel the interfering signal for user 1, in Fig. 7 user 2 needs to cancel the pre-coded version of the signals intended for both user 1 and user 3.

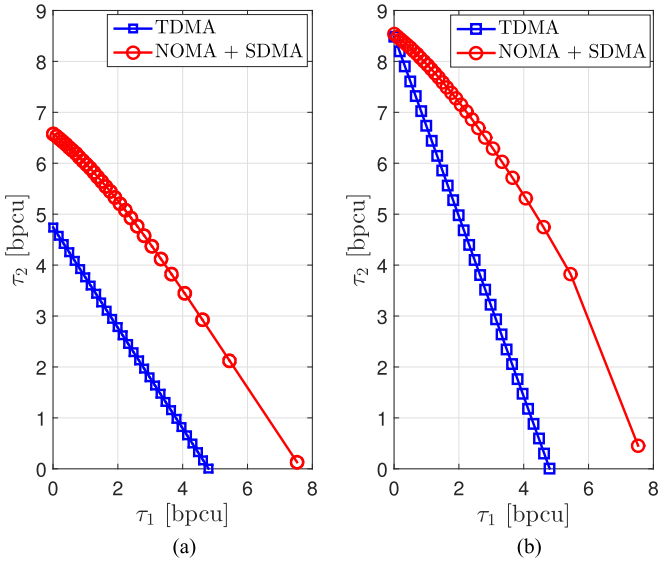

Fig. 8. Shannon spectral efficiency comparison between hybrid NOMA/SDMA and TDMA in a LiFi network setup (two-attocell example): (a) user 1 and user 2 are both near the cell edge; (b) user 1 is near the cell edge while user 2 is near the cell center.

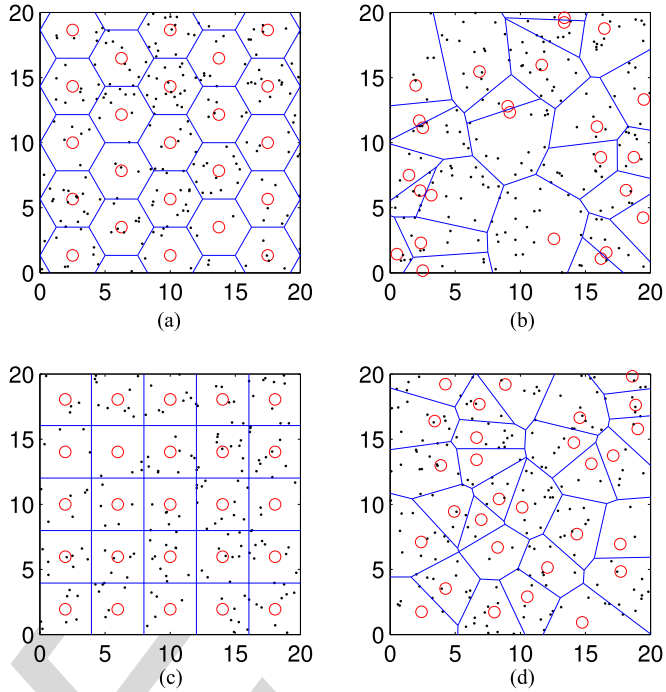

Fig. 9. A room of size 20 m $\times$ 20 m is considered. The circles in the figure represent the positions of the optical APs, which are also the room lights, while the dots represent the positions of the terminals which can be smartphones or 'things'. Different deployment scenario studied: (a) Hexagonal network model. (b) PPP network model. (c) square network model. (d) HCPP network model.

As shown in Fig. 8, the performance of NOMA in combination with SDMA is simulated in a LiFi network with two neighbouring attocells. The setup for LiFi APs and users is similar as the one shown in Fig. 7, where the locations of user 1, 3 and 4 are fixed while user 2 is moved from the cell edge [see Fig. 8(a)] to the cell center [see Fig. 8(b)]. The theoretical Shannon spectral efficiency is computed for both users in attocell 1. As shown in Fig. 8, if no intelligent interference management techniques are used, the performance of TDMA in a typical LiFi network is severely affected by inter-cell interference. On the other hand, the throughput of a LiFi network can be greatly increased by using NOMA and SDMA techniques.

VI. Modelling LiFi Networks

In a LiFi attocell network, the placement of APs affects the system performance. The light signal from a neighbouring AP causes interference which limits the SINR. Due to the use of LEDs, coherent transmission is not possible, and data has to be encoded by means of IM/DD. As a consequence, the frequencies used are between zero and typically 20 MHz for phosphor-coded commercial white LEDs assuming a blue filter at the receiver, and between 60–100 MHz for micro-LEDs. In order to provide multiuser access and mitigate CCI, the available bandwidth can be divided and shared among different optical APs according to the well-known frequency reuse concept [39]. Frequency reuse is modelled with a parameter Δ. For example, $\Delta = 3$ means that the available modulation bandwidth is divided into three equal parts and each part is assigned to an AP in a way that the geometric re-use distance of the same part of the bandwidth is maximised. Since lighting and wireless data communication are combined the placement of the optical APs is mainly determined by the lighting design. The effect of the location of APs is evaluated for four different scenarios as shown in Fig. 9. The models developed for cellular RF networks are used because the principal optimisation objectives are similar, namely, complete and uniform signal coverage. Similarly, lighting in home and office environments is designed to illuminate the entire space in a uniform manner [40]. Fig. 9(a) shows the conventional hexagonal topology widely used in RF cellular networks. This is an idealised model, in which APs are placed deterministically to form a hexagonal shaped Voronoi tessellation. Another type of the deterministic model is the square lattice topology, shown in Fig. 9(c), where the formed Voronoi cells have squared shapes. Compared with the hexagonal model, the square model is more suitable to model the regular lighting condition in large offices and public areas. However, the indoor environment typically contains a large number of 'statically random' APs, such as ceiling luminaries, desktop lamps and even LED screens. Therefore, using deterministic models to analyse the performance of such a network is no longer realistic. Spatial point process provides more accurate and tractable solutions for network interference modelling. The homogeneous Poisson point process (PPP) [41] is the most commonly used spatial model studied in ad hoc networks, in which the number of APs is assumed to follow the Poisson distribution and the APs are geographically independent of each other. The use of the PPP model for LiFi networks is shown in Fig. 9(b). However, in PPP two APs can be arbitrarily close to each other, which is unrealistic. Fig. 9(d) shows the Matérn type I hard-core point process (HCPP) deployment scenario, which includes an additional parameter c that controls the minimum separation between any two APs in order to address

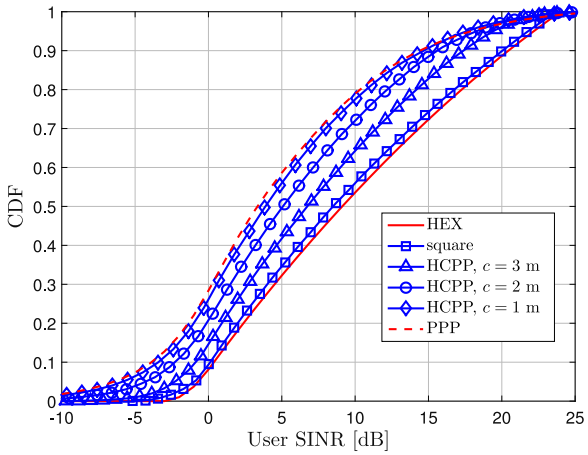

Fig. 10. Cumulative density function (CDF) comparison of the SINR for different network deployments. The BS density of each system is 0.0353 APs/m^2, and full frequency re-use is assumed, i.e. $\Delta = 1$. Other parameters are listed in Table I.

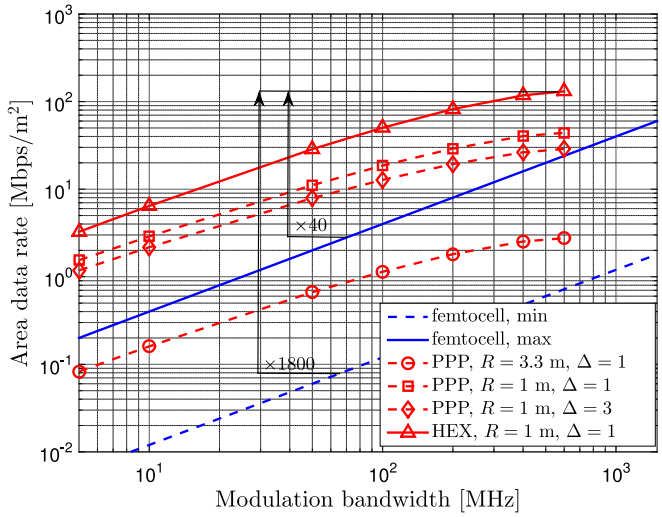

Fig. 11. Area data rate of a LiFi attocell network assuming different deployment scenarios, and comparison with state-of-the-art RF femtocell networks. The micro-LED as used in [3] is considered, whose 3-dB bandwidth is 60 MHz. Note, bit and power loading are used in DCO-OFDM, and the modulation bandwidth is significantly larger than the device bandwidth as there are no bandwidth limitations. This is because LiFi uses free and unlicensed spectrum.

the limitation of the PPP model in Fig. 9(b) [42]. These four models represent many specific lighting deployment scenarios. Experimental validation of this is being undertaken. Random user locations are considered in this work. Fig. 10 shows the CDF of the SINR for the different network topologies in Fig. 9. For all scenarios an AP density of 0.0353 APs/m^2 is considered. The optical output power of the LiFi AP is set so that the average illuminance in the room is at least 500 lx for reading purposes [40]. The rest of the system parameters are listed in Table I. From Fig. 10, it can be seen that the SINR of an APs deployment on a hexagonal lattice gives the best performance, followed by the deployment on a square lattice. Similar to the conclusions in [41], the SINR performance of a random PPP network results in the worst performance. If a minimum distance between APs is enforced by using the HCPP model, the SINR performance improves as is expected. The results show that the performance of a LiFi optical attocell network can vary significantly. Assuming a minimum SINR of 3 dB for data transmission with acceptable BER, the probability that this would be achieved can vary between 50% and 75%.

The data rate performance is also evaluated and compared with state-of-the-art RF femtocell networks. Optical attocell networks exploit the ability of LiFi to achieve a massive spatial reuse because the typical cell radius, R, is 1–4 m enabling a room to have multiple independent LiFi APs. In contrast, femtocells typically have an order of magnitude larger cell radius [43]. To demonstrate the high data density achieved by an optical attocell system, the area data rate, s_{area}, is used, and this is defined as:

$$s_{\text{area}} = \frac{s}{A_{\text{cell}}}, \tag{2}$$

where A_{cell} is the average cell area defined as the coverage area of a single AP, and s is the average throughput of a single cell. The throughput is obtained from the SINR using adaptive modulation and coding tables [44]. The division by the cell area allows for a normalisation for different cell areas, and is related to the area spectral efficiency (ASE). Fig. 11 shows the area data rate performance of optical attocell networks and femtocell networks against channel bandwidth, as LEDs provide a freely available spectrum. Also, Fig. 11 shows the potential if future LED devices are improved in terms of their bandwidth. The results of the femtocell network are taken from [43], [45]–[47]. The indoor ASE achieved by the femtocell network is generally in the range from 0.03 to 0.0012 bps/Hz/m^2. Therefore, this ASE range is used to calculate a minimum and maximum area data rate for the benchmark femtocell network. From Fig. 11 it can be concluded that i) the LiFi attocell network could achieve 40–1800 higher area data rate compared with femtocell networks; ii) the best femtocell performance would require a total channel bandwidth of 600 MHz to achieve the same performance of a LiFi attocell network with PPP-based AP deployment, frequency reuse of 3 and cell radius of 1 m; iii) when the LiFi AP cell coverage is large ($R = 3.3$ m, $A_{\text{cell}} = 34.2$ m^2), the AP deployment is PPP random, and full frequency reuse ($\Delta = 1$), the LiFi attocell area data rate performance is within the reported range of femtocell networks, and also closer to the maximum reported performance; and iv) in all cases, the LiFi attocell network enhances the wireless performance significantly, and for the considered office of 400 m^2, the additional maximum throughput is in the range of 12–48 Gb/s.

VII. Hybrid LiFi/WiFi Networks

As shown in VI, LiFi networks can achieve high throughput with a dense deployment of optical APs. However, referring to Fig. 10, the spatial distribution of the data rates fluctuates due to the CCI. In order to augment the system performance and to guarantee equally high Quality of Service (QoS) among users, an additional Wireless-Fidelity (WiFi) overlay can be deployed.

Due to the different spectra used by LiFi and WiFi there is no interference among these systems. Therefore, a hybrid LiFi/WiFi network is capable of achieving the sum throughput of both LiFi and WiFi stand-alone networks. According to the IEEE 802.11ad standard, the latest WiFi protocol provided by Wireless Gigabit Alliance (WiGig) enables devices to operate in three centre frequencies (2.4, 5 and 60 GHz), and WiGig can achieve a total data rate up to 7 Gb/s [48]. At the same time, recent studies show that 3 Gb/s can be achieved with a single micro-LED [3], and that it is possible to go up to 100 Gb/s with laser LEDs combined with an optical diffuser to achieve broad illumination [49]. Because there is the potential for a large number of LiFi APs in an indoor environment when using existing lighting infrastructures, a LiFi network can achieve high ASE [50] as shown in Section VI. By considering a hybrid LiFi/WiFi system, users at all possible locations within an enlarged coverage area can benefit from significantly enhanced user throughput and QoS. The WiFi system benefits from reduced contention and resulting spectrum efficiency losses, as well as RF spectrum relief due to the offload into the free light spectrum, while LiFi benefits from coverage at dead spots.

A. Hybrid LiFi/WiFi System Model

A hybrid LiFi/WiFi network consists of bi-directional communication transceivers for both LiFi and WiFi links and also a central unit (CU), which integrates these two different networks. All of the users in the hybrid network are equipped with a RF antenna and a PD for both WiFi and LiFi signals. The CU monitors the whole network regularly in a short period, and receives the CSI feedback of users for LiFi and WiFi links. Following that, each user is assigned to a suitable AP by the CU, and the communication RA for users connected to each AP is determined. In this section, the system load balancing for downlink hybrid LiFi/WiFi network is studied. The Lambertian channel model is used for LoS LiFi links [51], and the dispersive optical channel is modelled by an approximation given in [52]. In addition, DCO-OFDM and adaptive bit loading are employed to enhance the spectral efficiency [53]. LiFi APs share the same modulation bandwidth. Therefore, users in the overlapping area of LiFi attocells experience inter-user interference. The WiFi AP is assumed to cover the entire indoor area, and the WiFi channel model is based on IEEE 802.11g [54]. The hybrid system offers significant benefits in terms of capacity, robustness, security and reliability which are important metrics in a massively growing internet in terms of number of devices connected and data volumes transmitted. The Internet-of-Things (IoT) will be one of the sources of demand for this growth.

B. System Load Balancing

Hybrid LiFi/WiFi networks can benefit from an effective design of a load balancing technique. Due to multiple APs and multiuser communications, a system load balancing scheme should address two main issues, AP assignment and RA, which can be formulated as a joint optimisation problem. A utility function can be applied to combine these two optimization objects. The logarithmic utility function that achieves proportional fairness for users is widely used due to its simplicity and practicability [53]. It is shown in [53] that all of the users served by each AP share the time resource equally when the optimal load balancing is achieved. Figs. 12 and 13 show the distribution of users using the random waypoint (RWP) model [55] and they are served by different APs in the hybrid LiFi/WiFi network with 120 Mb/s and 1 Gb/s WiFi throughput, respectively. The receiver field of view (FoV) for LiFi signals is set to 60°, and other parameters are listed in Table I. The WiFi AP is assumed to provide a uniform distribution of achievable data rate in the considered scenario. As shown, users in the overlap area of LiFi

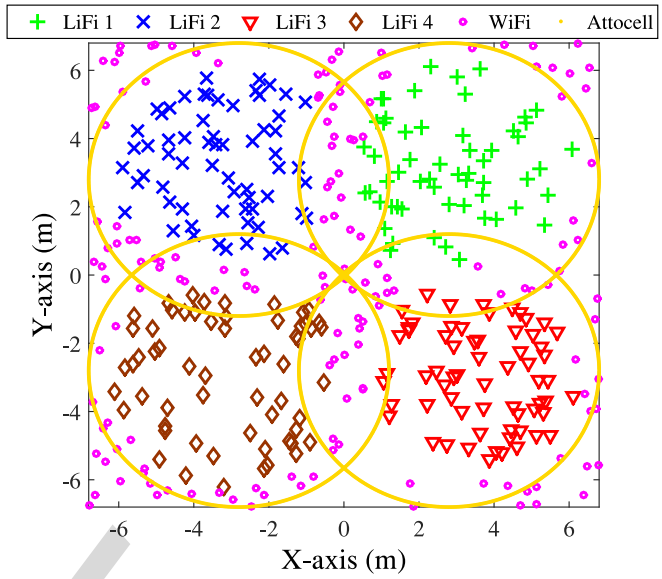

Fig. 12. Distribution of users served by different APs with optical CCI considered. 4 LiFi APs and 1 WiFi AP are deployed in the hybrid network. The WiFi throughput is 120 Mb/s.

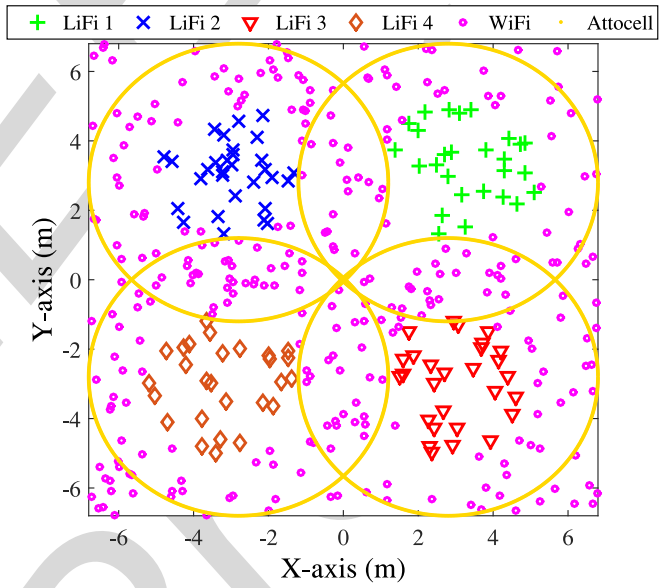

Fig. 13. Distribution of users served by different APs with optical CCI considered. Four LiFi APs and one WiFi AP are deployed in the hybrid network. The WiFi throughput is 1 Gb/s.

attocells are more likely to select the WiFi AP due to the effect of optical CCI. Also, the service area of each LiFi AP decreases with an increase in WiFi throughput. The LiFi service area in Fig. 13 is smaller than that in Fig. 12 due to the WiFi throughput enhancement. Since users close to the centre of attocells experience better LiFi channels, the LiFi throughput increases when the WiFi throughput is improved [53]. This indicates that both the WiFi and LiFi throughput performances in the hybrid network are mutually dependent when using a cross-domain load balancing technique, despite their fully independent spectrum use.

C. Dynamic Handover

In practical scenarios, the CSI of both LiFi and WiFi links is time-varying due to the random movement of users. According to Figs. 12 and 13, users outside the LiFi attocells are served by the WiFi AP. If a mobile user, who is currently served by WiFi, senses a stronger LiFi signal, it will transfer to the LiFi network. Thus, in a hybrid LiFi/WiFi network, mobile users may experience frequent handovers. In addition, a handover resulting from user movement may cause some knock-on handover effects. For example, if a user is transferred from LiFi to WiFi, it will increase the load in the corresponding WiFi cell. Other users served by this WiFi AP may have to be transferred to neighbouring WiFi APs, or reduce achievable data rates. Also, due to the decrease in the load of the LiFi attocell, resources are freed up to enhance the data rates for existing users. Moreover, blockage and/or varying receive angle may cause a transient CSI decrease of LiFi channels, which could prompt ping-pong handover effects between LiFi and WiFi APs. On average, the handover process takes about 30–3000 ms [56], [57], depending on the algorithms used. This additional signalling overhead decreases the overall system throughput. In order to mitigate the influence of handover, a fuzzy logic (FL) based dynamic handover scheme is proposed. The FL method yields a truth value in a certain range instead of making a hard decision. In general, there are four steps in a FL system: fuzzification, rule evaluation, defuzzification and decision making [58], [59]. In a FL system, a chain of input information, e.g., instantaneous and average SINR of LiFi links, user speed and required data rate of users, is combined to determine a suitable load balancing solution, with the aim of reducing possible handover and improve the system throughput. In the fuzzification step, the inputs of the FL system are converted into crisp values with membership functions (MFs). The triangular, sigmoidal, and sigmoidal product functions are generally applied as the MFs [59]. In the process of rule evaluation, the crisp values in the fuzzy set of inputs are combined based on the fuzzy rules to determine the 'score' of the outputs. For example, users with low instantaneous LiFi SINR, but high average SINR can still be allocated to a LiFi AP because the low LiFi SINR is probably caused by transient LoS blockage of objects. These rules are heuristic. Essentially, they are intuitive guidelines on the reason a specific user is allocated to a LiFi AP or a WiFi AP. The result of the rule evaluation step yields an output set for each user, which contains certain crisp values for each user and represents how strongly this user should be allocated to the LiFi AP or the WiFi AP. In the defuzzification step, the final score of AP allocation for each user is determined. Specifically, the centre of gravity of the fuzzy set obtained in the rule evaluation step is calculated for the final score [58]. Eventually, in the step of decision making, the AP allocation is executed by the CU according to the final score of each user, and proportional fairness scheduling is used for RA in each cell.

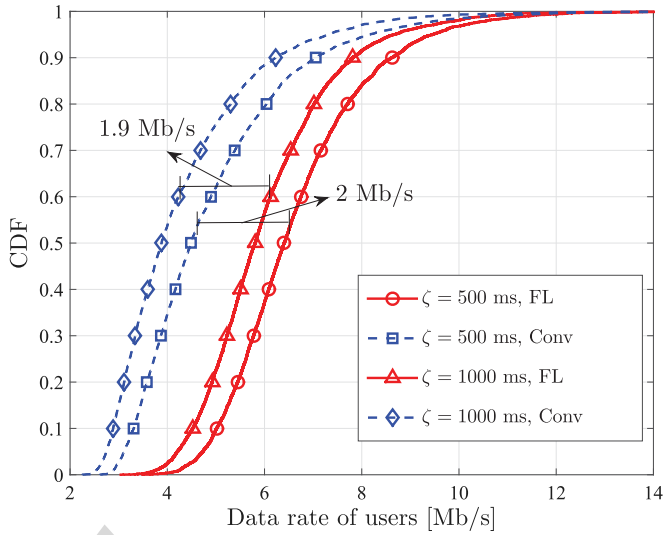

Fig. 14. Comparison of the data rate performance of the FL based dynamic handover scheme and the conventional load balancing algorithm in the hybrid LiFi/WiFi network. The simulation scenario includes 36 LiFi APs and one WiFi AP. The setup of the hybrid network follows the model given in VII-B. ζ is the average handover overhead.

The proposed FL handover scheme can significantly reduce the number of handovers and achieve increased data rate. The comparison of the data rate performance between the FL based dynamic handover scheme and the conventional load balancing scheme without handover enhancement is shown in Fig. 14. The user mobility follows the RWP model, given in [53]. The conventional scheme is based only on the SINR of LiFi and WiFi links, shown in [60]. In the legend of 14, the FL-based scheme and the conventional scheme are denoted by "FL" and "Conv," respectively. As shown, the data rate performance of the FL scheme is better than that with the conventional one. In the case of 200 users and 500 ms average handover overhead, the gain of user data rate is approximately 2 Mb/s. This means that the proposed handover scheme can reduce data rate losses in the hybrid LiFi/WiFi network. The user data rates of both schemes decrease with an increase in the handover overhead. When the overhead time is set to 1000 ms, the gain achieved by the proposed scheme slightly decreases to 1.9 Mb/s. In practical indoor scenarios, the FL based dynamic load balancing scheme can improve the data rate performance by 40% compared with an SINR-based state-of-the-art technique.

VIII. Summary and Conclusion

More than 15 years of research in physical layer techniques for LED-based VLC has provided the fundamental solutions

to develop LiFi attocell networks that are capable of achieving magnitudes of higher data rates per unit area compared with state-of-the-art RF small cell solutions. The achievable performances in terms of user data rates, number of users served and increase in total traffic are well aligned with 5G key performance indicators. A key factor enabling this is the radical reduction of cell sizes, and this is possible by using the existing infrastructures through the combination of LED lighting and wireless data networking. The new wireless LiFi networking paradigm offers performance enhancements that are not only aimed for by 5G initiatives, but also due to the ubiquitous use of LEDs, that will provide an infrastructure for the emerging IoT. It was one of the goals of this paper to shed light on the difference between VLC and LiFi. Moving on, this paper also showed and discussed the key research areas that are required to realise LiFi attocell networks. It summarised the well researched areas such as digital modulation techniques using LEDs, and provided new solutions to those areas which are key to LiFi networks such as multiuser access, LiFi attocell network analysis under various network deployment scenarios. Moreover, it provided results that demonstrated that load balancing techniques in hybrid LiFi/WiFi networks can achieve better total performances than sum performance of separate WiFi and LiFi networks. This provides evidence for the claim that LiFi, when considered as a complementary wireless networking technique, can not only provide additional free and vast wireless capacity, but also contribute to enhancing the spectrum efficiency of existing RF networks. In addition, this paper presented for the first time LiFi transmitter and receiver ASICs for miniaturised transceivers that are capable of $1\ \mathrm{Gb/s}$ transmission. The ASICs can be integrated into mobile terminals, "things" and wearables to realise LiFi attocell networks and provide the required connectivity to realise the IoT .

REFERENCES

[1] S. Dimitrov and H. Haas, *Principles of LED Light Communications: Towards Networked Li-Fi*. Cambridge, U.K.: Cambridge Univ. Press, Mar. 2015.

[2] H. Haas. (2011, Aug.). Wireless data from every light bulb. TED Website. [Online]. Available: http://bit.ly/tedvlc

[3] D. Tsonev, H. Chun, S. Rajbhandari, J. McKendry, S. Videv, E. Gu, M. Haji, S. Watson, A. Kelly, G. Faulkner, M. Dawson, H. Haas, and D. O'Brien, "A 3-Gb/s single-LED OFDM-based wireless VLC link using a gallium nitride μLED," *IEEE Photon. Technol. Lett.*, vol. 26, no. 7, pp. 637–640, Apr. 2014.

[4] S. Dimitrov and H. Haas, "Information rate of OFDM-based optical wireless communication systems with nonlinear distortion," *IEEE J. Lightw. Technol.*, vol. 31, no. 6, pp. 918–929, Mar. 2013.

[5] H. Haas, "High-speed wireless networking using visible light," SPIE Newsroom, Apr. 19, 2013, doi: 10.1117/2.1201304.004773.

[6] H. Haas and C. Chen, "What is LiFi?" in *Proc. 41st Eur. Conf. Opt. Commun.*, Valencia, Spain, Sep. 27, 2015–Oct. 1, 2015, pp. 1–3, doi: 10.1109/ECOC.2015.7341879.

[7] S. Rajagopal, R. Roberts, and S.-K. Lim, "IEEE 802.15.7 visible light communication: Modulation schemes and dimming support," *IEEE Commun. Mag.*, vol. 50, no. 3, pp. 72–82, Mar. 2012.

[8] E. Sarbazi, M. Uysal, M. Abdallah, and K. Qaraqe, "Ray tracing based channel modeling for visible light communications," in *Proc. 22nd Signal Process. Commun. Appl. Conf.*, Apr. 2014, pp. 702–705.

[9] A. Farid and S. Hranilovic, "Capacity bounds for wireless optical intensity channels with Gaussian noise," *IEEE Trans. Inf. Theory*, vol. 56, no. 12, pp. 6066–6077, Dec. 2010.

[10] B. Rofoee, K. Katsalis, Y. Yan, Y. Shu, T. Korakis, L. Tassiulas, A. Tzanakaki, G. Zervas, and D. Simeonidou, "First demonstration of service-differentiated converged optical sub-Wavelength and LTE/WiFiNetworks over GEAN," in *Proc. Opt. Fiber Commun. Conf. Exhib.*, Mar. 2015, pp. 1–3.

[11] J. M. Kahn and J. R. Barry, "Wireless infrared communications," *Proc. IEEE*, vol. 85, no. 2, pp. 265–298, Feb. 1997.

[12] IEEE Std. 802.15.7-2011, *IEEE Standard for Local and Metropolitan Area Networks, Part 15.7: Short-Range Wireless Optical Communication Using Visible Light*, IEEE Std., 2011.

[13] R. Mesleh, H. Elgala, and H. Haas, "Optical spatial modulation," *IEEE/OSA J. Opt. Commun. Netw.*, vol. 3, no. 3, pp. 234–244, Mar. 2011.

[14] F.-M. Wu, C.-T. Lin, C.-C. Wei, C.-W. Chen, H.-T. Huang, and C.-H. Ho, "1.1-Gb/s white-LED-based visible light communication Employing carrier-less amplitude and phase modulation," *IEEE Photon. Technol. Lett.*, vol. 24, no. 19, pp. 1730–1732, Oct. 2012.

[15] T. Komine, S. Haruyama, and M. Nakagawa, "Performance evaluation of narrowband OFDM on integrated system of power line communication and visible light wireless communication," in *Proc. Int. Symp. Wireless Pervasive Comput.*, Jan. 2006, doi: 10.1109/ISWPC.2006.1613633.

[16] M. Z. Afgani, H. Haas, H. Elgala, and D. Knipp, "Visible light communication using OFDM," in *Proc. 2nd Int. Conf. Testbeds Res. Infrastruct. Develop. Netw. Commun.*, 2006, p. 134, doi: 10.1109/TRIDNT.2006.1649137.

[17] J. Armstrong and A. Lowery, "Power efficient optical OFDM," *Electron. Lett.*, vol. 42, no. 6, pp. 370–372, Mar. 16, 2006.

[18] S. Dissanayake, K. Panta, and J. Armstrong, "A novel technique to simultaneously transmit ACO-OFDM and DCO-OFDM in IM/DD systems," in *Proc. IEEE GLOBECOM Workshops*, Houston, TX, USA, Dec. 5–9, 2011, pp. 782–786.

[19] H. Elgala and T. D. C. Little, "Reverse polarity optical-OFDM (RPO-OFDM): Dimming compatible OFDM for Gigabit VLC links," *Opt. Exp.*, vol. 21, no. 20, pp. 24288–24299, 2013.

[20] S. C. J. Lee, S. Randel, F. Breyer, and A. M. J. Koonen, "PAM-DMT for intensity-modulated and direct-detection optical communication systems," *IEEE Photon. Technol. Lett.*, vol. 21, no. 23, pp. 1749–1751, Dec. 2009.

[21] Q. Wang, Z. Wang, and L. Dai, "Asymmetrical hybrid optical OFDM for visible light communications with dimming control," *IEEE Photon. Technol. Lett.*, vol. 27, no. 9, pp. 974–977, May 2015.

[22] M. Mossaad, S. Hranilovic, and L. Lampe, "Visible light communications using OFDM and multiple LEDs," *IEEE Trans. Commun.*, vol. 63, no. 11, pp. 4304–4313, Nov. 2015.

[23] N. Fernando, Y. Hong, and E. Viterbo, "Flip-OFDM for unipolar communication systems," *IEEE Trans. Commun.*, vol. 60, no. 12, pp. 3726–3733, Dec. 2012.

[24] D. Tsonev, S. Sinanović, and H. Haas, "Novel unipolar orthogonal frequency Division multiplexing (U-OFDM) for optical wireless," presented at the Vehicular Technology Conf., Yokohama, Japan, May 6–9, 2012.

[25] D. Tsonev, S. Videv, and H. Haas, "Unlocking spectral efficiency in intensity modulation and direct detection systems," *IEEE J. Sel. Areas Commun.*, vol. 33, no. 9, pp. 1758–1770, Sep. 2015.

[26] M. Noshad and M. Brandt-Pearce, "Hadamard coded Modulation: An alternative to OFDM for wireless optical communications," in *Proc. IEEE Global Commun. Conf.*, Dec. 2014, pp. 2102–2107.

[27] E. Monteiro and S. Hranilovic, "Constellation design for color-shift keying using interior point methods," in *Proc. IEEE Globecom Workshops*, Dec. 2012, pp. 1224–1228.

[28] P. M. Butala, J. C. Chau, and T. D. C. Little, "Metameric modulation for diffuse visible light communications with constant ambient lighting," in *Proc. Int. Workshop Opt. Wireless Commun.*, Pisa, Italy, Oct. 2012, pp. 1–3.

[29] K.-I. Ahn and J. K. Kwon, "Color intensity modulation for multicolored visible light communications," *IEEE Photon. Technol. Lett.*, vol. 24, no. 24, pp. 2254–2257, Dec. 2012.

[30] B. Schafferer and R. Adams, "A 3V CMOS 400 mW 14b 1.4 GS/s DAC for multi-carrier applications," in *Proc. IEEE Int. Solid-State Circuits Conf.*, Feb. 2004, pp. 360–532.

[31] A. Jalajakumari, K. Cameron, R. Henderson, D. Tsonev, and H. Haas, "An energy efficient high-speed digital LED driver for visible light communications," in *Proc. IEEE Int. Conf. Commun.*, Jun. 2015, pp. 5054–5059.

[32] Z. Chen, D. Tsonev, and H. Haas, "A novel double-source cell configuration for indoor optical attocell networks," presented at the Global Telecommunication Conf., Austin, TX, USA, Dec. 8–12, 2014.

[33] S. Rajbhandari, H. Chun, G. Faulkner, K. Cameron, A. V. N. Jalajakumari, R. Henderson, D. Tsonev, M. Ijaz, Z. Chen, H. Haas, E. Xie, J. J. D. McKendry, J. Herrnsdorf, E. Gu, M. D. Dawson, and D. O'Brien,

"High-speed integrated visible light communication system: Device constraints and design considerations," *IEEE J. Sel. Areas Commun.*, vol. 33, no. 9, pp. 1750–1757, Sep. 2015.
[34] Z. Chen, N. Serafimovski, and H. Haas, "Angle diversity for an indoor cellular visible light communication system," presented at the Vehicular Technology Conf., Seoul, Korea, May 18–21, 2014.
[35] Z. Chen and H. Haas, "Space division multiple access in visible light communications," in *Proc. IEEE Int. Conf. Commun.*, London, U.K., Jun. 2015, pp. 5115–5119.
[36] Y. Saito, Y. Kishiyama, A. Benjebbour, T. Nakamura, A. Li, and K. Higuchi, "Non-orthogonal multiple access (NOMA) for cellular future radio access," in *Proc. IEEE Veh. Technol. Conf.*, Dresden, Germany, Jun. 2013, pp. 1–5.
[37] L. Yin, X. Wu, and H. Haas, "On the performance of non-orthogonal multiple access in visible light communication," in *Proc. IEEE 26th Annu. Symp. Personal, Indoor Mobile Radio Commun.*, Hong Kong, Sep. 2015, pp. 1376–1381.
[38] L. Dai, B. Wang, Y. Yuan, S. Han, C.-L. I, and Z. Wang, "Non-orthogonal multiple access for 5G: Solutions, challenges, opportunities, and future research trends," *IEEE Commun. Mag.*, vol. 53, no. 9, pp. 74–81, Sep. 2015.
[39] V. Donald, "Advanced mobile phone service: The cellular concept," *Bell Syst. Tech. J.*, vol. 58, no. 1, pp. 15–41, Jan. 1979.
[40] *Lighting of Indoor Work Places*, European Standard EN 12464-1, Jan. 2009.
[41] J. Andrews, F. Baccelli, and R. Ganti, "A tractable approach to coverage and rate in cellular networks," *IEEE Trans. Commun.*, vol. 59, no. 11, pp. 3122–3134, Nov. 2011.
[42] D. Stoyan, W. S. Kendall, and J. Mecke, *Stochastic Geometry and its Applications*, 2nd ed. Hoboken, NJ, USA: Wiley, 1995.
[43] V. Chandrasekhar, J. Andrews, and A. Gatherer, "Femtocell networks: A survey," *IEEE Commun. Mag.*, vol. 46, no. 9, pp. 59–67, Sep. 2008.
[44] F. Xiong, *Digital Modulation Techniques*, 2nd ed. Norwood, MA, USA: Artech House, 2006.
[45] P. Chandhar and S. Das, "Area spectral efficiency of co-channel deployed OFDMA femtocell networks," *IEEE Trans. Wireless Commun.*, vol. 13, no. 7, pp. 3524–3538, Jul. 2014.
[46] H.-S. Jo, P. Xia, and J. Andrews, "Downlink femtocell networks: Open or closed?" in *Proc. IEEE Int. Commun. Conf.*, Jun. 2011, pp. 1–5.
[47] W. C. Cheung, T. Quek, and M. Kountouris, "Throughput optimization, spectrum allocation, and access control in two-tier femtocell networks," *IEEE J. Sel. Areas Commun.*, vol. 30, no. 3, pp. 561–574, Apr. 2012.
[48] C. Hansen, "WiGig: Multi-Gigabit wireless communications in the 60 GHz band," *IEEE Wireless Commun.*, vol. 18, no. 6, pp. 6–7, Dec. 2011.
[49] D. Tsonev, S. Videv, and H. Haas. (2015, Jan.). Towards a 100 Gb/s visible light wireless access network. *Opt. Exp.* [Online]. *23(2)*, pp. 1627–1637. Available: http://www.opticsexpress.org/abstract.cfm?URI=oe-23-2-1627
[50] I. Stefan, H. Burchardt, and H. Haas, "Area spectral efficiency performance comparison between VLC and RF femtocell networks," in *Proc. IEEE Int. Conf. Commun.*, Budapest, Hungary, Jun. 9–13, 2013, pp. 1–5.
[51] J. Kahn and J. Barry, "Wireless infrared communications," *Proc. IEEE*, vol. 85, no. 2, pp. 265–298, Feb. 1997.
[52] V. Jungnickel, V. Pohl, S. Nonnig, and C. Von Helmolt, "A physical model of the wireless infrared communication channel," *IEEE J. Sel. Areas Commun.*, vol. 20, no. 3, pp. 631–640, Apr. 2002.
[53] Y. Wang and H. Haas, "Dynamic load balancing with handover in hybrid Li-Fi and Wi-Fi networks," *J. Lightw. Technol.*, vol. 33, no. 22, pp. 4671–4682, Nov. 2015.
[54] E. Perahia and R. Stacey, *Next Generation Wireless LAN: 802.11n and 802.11ac*. Cambridge, U.K.: Cambridge Univ. Press, 2013.
[55] D. B. Johnson and D. A. Maltz, "Dynamic source routing in Ad Hoc wireless networks," *Mobile Comput.*, pp. 153–181, 1996.
[56] M. Kassab, M. Bonnin, and A. Belghith, "Fast and secure handover in WLANs: An Evaluation of the signaling overhead," in *Proc. IEEE Consum. Commun. Netw. Conf.*, Las Vegas, NV, USA, Jan. 2008, pp. 770–775.
[57] A. M. Vegni and T. D. C. Little, "Handover in VLC systems with cooperating mobile devices," in *Proc. Int. Conf. Comput. Netw. Commun.*, Maui, HI, USA, Jan. 2012, pp. 126–130.
[58] X. Wu, M. Safari, and H. Haas, "3-State fuzzy logic game on resource allocation for small cell networks," presented at the IEEE Annu. Symp. Personal, Indoor Mobile Radio Communication, Hong Kong, Sep. 2015.
[59] H. Burchardt, S. Sinanovic, Z. Bharucha, and H. Haas, "Distributed and autonomous resource and power allocation for wireless networks," *IEEE Trans. Commun.*, vol. 61, no. 7, pp. 2758–2771, Jul. 2013.
[60] Y. Wang, D. Basnayaka, and H. Hass, "Dynamic load balancing for hybrid Li-Fi and RF indoor networks," in *Proc. IEEE Int. Conf. Commun. Workshop*, London, U.K., Jun. 2015, pp. 1422–1427.

Harald Haas (S'98–A'00–M'03) received the Ph.D. degree from the University of Edinburgh, Edinburgh, U.K., in 2001. He currently holds the Chair of Mobile Communications at the University of Edinburgh, and is the cofounder and Chief Scientific Officer of pureLiFi, Ltd., as well as the Director of the LiFi Research and Development Centre at the University of Edinburgh. His main research interests include optical wireless communications, hybrid optical wireless and RF communications, spatial modulation, and interference coordination in wireless networks. He first introduced and coined spatial modulation and LiFi. LiFi was listed among the 50 best inventions in *TIME Magazine* 2011. He was an Invited Speaker at TED Global 2011, and his talk: "Wireless Data From Every Light Bulb" has been watched online 2.2 million times. He gave a second TED Global lecture in 2015 on the use of solar cells as LiFi data detectors and energy harvesters. This has been viewed online more than 1 million times. He holds 31 patents and has more than 30 pending patent applications. He has published 300 conference and journal papers including a paper in *Science*. He coauthored a book entitled: *Principles of LED Light Communications Towards Networked Li-Fi* (Cambridge, U.K.: Cambridge Univ. Press, 2015). He received recent Best Paper awards at the IEEE Vehicular Technology Conference (VTC-Fall) in Las Vegas in 2013, and VTC-Spring in Glasgow in 2015. He received the EURASIP Best Paper Award for the *Journal on Wireless Communications and Networking* in 2015, and the Jack Neubauer Memorial Award of the IEEE Vehicular Technology Society. In 2012, he received the prestigious Established Career Fellowship from the Engineering and Physical Sciences Research Council (EPSRC) within Information and Communications Technology in the U.K. He also received the Tam Dalyell Prize 2013 awarded by the University of Edinburgh for excellence in engaging the public with science. In 2014, he was selected by EPSRC as one of ten recognising inspirational scientists and engineers leaders in the U.K.

Liang Yin (S'15) received the B.Eng. degree (first class Hons.) in electronics and electrical engineering from the University of Edinburgh, Edinburgh, U.K., in 2014, where he is currently working toward the Ph.D. degree in electrical engineering. His research interests include visible light communication, indoor visible light positioning, and multiuser networking.

Yunlu Wang received the B.Eng. degree in telecommunication engineering from the Beijing University of Post and Telecommunications, Beijing, China, in 2011, and the M.Sc. degrees in digital communication and signal processing from the University of Edinburgh, Edinburgh, U.K., and in electronic and electrical engineering from Beihang University, China, in 2013. He is currently working toward the Ph.D. degree in electrical engineering at the University of Edinburgh. His research interests include visible light communication and radio frequency hybrid networking.

Cheng Chen (S'14) received the B.Eng. degree in electronic and electrical engineering from the University of Strathclyde, Glasgow, U.K., in 2011, and the M.Sc. degree in communications and signal processing from the Imperial College London, London, U.K., in 2012. He is currently working toward the Ph.D. degree in electrical engineering at the University of Edinburgh, Edinburgh, U.K. His research interests include visible light communication networking and interference mitigation.